Towards molecular spintronics

ALEXANDRE R. ROCHA[1], VíCTOR M. GARCíA-SUÁREZ[2], STEVE W. BAILEY[3], COLIN J. LAMBERT[3], JAIME FERRER[2] AND STEFANO SANVITO[1]*

[1]Physics Department, Trinity College, Dublin 2, Ireland
[2]Departamento de Física, Facultad de Ciencias, Universidad de Oviedo, 33007 Oviedo, Spain
[3]Department of Physics, Lancaster University, Lancaster, UK
*e-mail: sanvitos@tcd.ie

The ability to manipulate electron spin in organic molecular materials offers a new and extremely tantalizing route towards spin electronics, both from fundamental and technological points of view. This is mainly due to the unquestionable advantage of weak spin–orbit and hyperfine interactions in organic molecules, which leads to the possibility of preserving spin-coherence over times and distances much longer than in conventional metals or semiconductors. Here we demonstrate theoretically that organic spin valves, obtained by sandwiching an organic molecule between magnetic contacts, can show a large bias-dependent magnetoresistance and that this can be engineered by an appropriate choice of molecules and anchoring groups. Our results, obtained through a combination of state-of-the-art non-equilibrium transport methods and density functional theory, show that although the magnitude of the effect varies with the details of the molecule, large magnetoresistance can be found both in the tunnelling and the metallic limit.

In the search for large magnetoresistance in both the tunnelling and metallic regime, we analyse respectively *n*-alkane-dithiolate and 1,4-*n*-phenyl-dithiolate molecules. In the case of nickel contacts the first molecule shows tunnelling behaviour with the spin-polarization of the current mainly given by surface states at the interface between the nickel and the molecule. In contrast, in 1,4-*n*-phenyl-dithiolate the transport is by means of states extending across the whole molecule, which determine the spin-polarization of the junction. Our findings raise expectations for a chemical route to spintronics devices[1], where efficiency and performance can be engineered by the appropriate choice of molecules and end groups, thus integrating the two burgeoning fields of molecular- and spin-electronics.

There have been several investigations of spin-transport through organic molecules. These include carbon nanotube spin valves[2], hot electron coherent spin transfer across molecular bridges[3], spin-injection in π-conjugated molecules[4,5] and organic tunnelling junctions[6]. At the same time a few seminal theoretical studies on transport through 1,4-benzene-dithiolate molecular spin-valves[7,8] and molecular magnets[9] have appeared. Although these works demonstrate convincingly that spin-polarized currents can be injected into organic materials with reasonably high efficiency, there is a general lack of control over the magnetic response of the devices. Low yield in the device production[2], severe temperature- and bias-dependence of the magneto-transport properties[6], and large resistances[5] are serious limiting factors for future applications.

The origin of these disruptive effects lies in an incomplete knowledge and control of the binding properties between the organic materials and the magnetic electrodes and of their response to external magnetic and electric fields. These are crucial aspects determining the magneto-transport in a spin valve. For instance, in ordinary tunnel junctions the spin-polarization of the device is given by the electronic states at the interface between the magnetic electrodes and the insulator[10]. In molecular objects these are sensitive to the contact geometry, the molecular end-groups and the nature of the molecule, all of which leads to great variability in magnetoresistance. Consequently an increased understanding and control of these factors could open up the exciting prospect of chemically engineering the desired magnetic response.

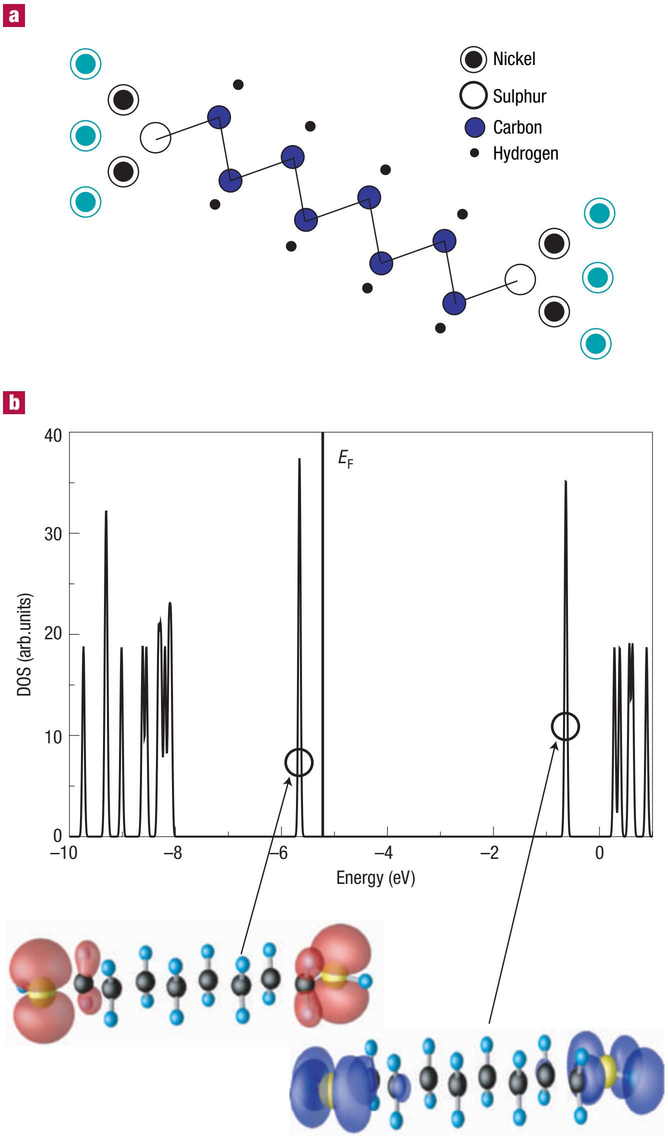

Figure 1. Structural and electronic properties of a Ni(001)/octane/Ni(001) spin-valve. a, Schematic structure of the octane molecule attached to (001) Ni surfaces. **b**, Density of states and charge-density isosurface plots for the relevant molecular states of the isolated octane–dithiol molecule. The highest 'circled' state is the LUMO for such an isolated molecule. Because isolated levels correspond to delta functions in the DOS, for display purposes and to aid comparison with Figs 3–5 we have artificially broadened the DOS by 0.1 eV.

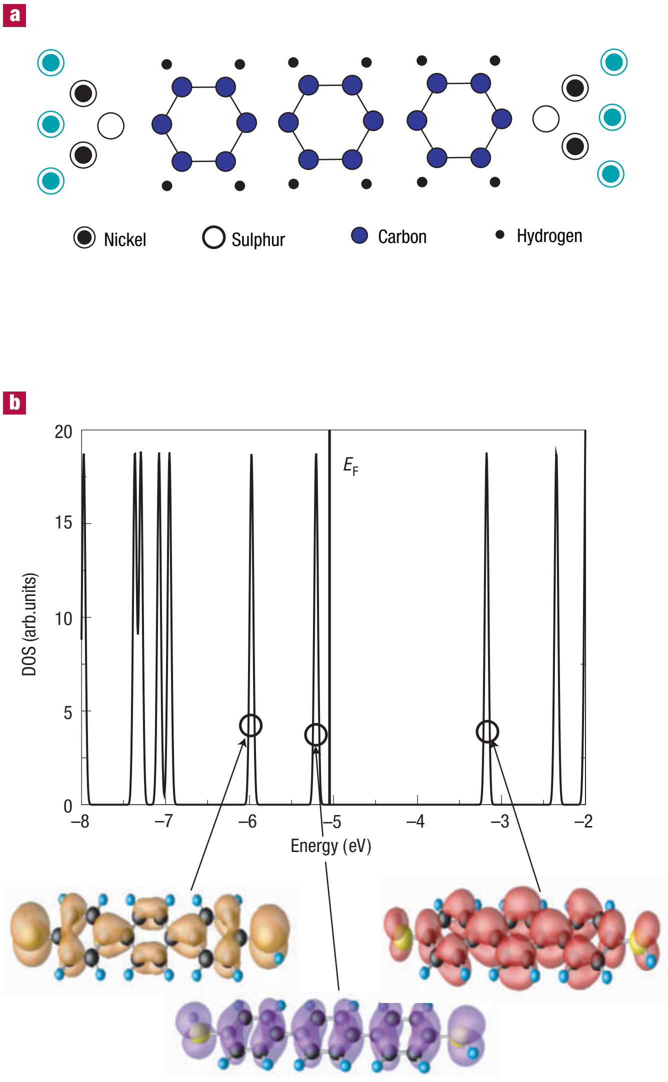

Figure 2 Structural and electronic properties of a Ni(001)/tricene/Ni(001) spin-valve. a, Schematic structure of the tricene molecule attached to (001) Ni surfaces. **b**, Density of states and charge-density isosurface plots for the relevant molecular states of the isolated tricene–dithiol molecule. The highest 'circled' state is the LUMO for such an isolated molecule. As in Fig. 1, we have artificially broadened the DOS by 0.1 eV.

Here we study two prototypical cases of molecular spin-valves, namely those obtained by sandwiching either 8-alkane-dithiolate (octane-dithiolate) or 1,4-3-phenyl-dithiolate (1,4-tricene-dithiolate) molecules between nickel contacts. The density of states and the charge-density isosurfaces of the highest occupied and lowest unoccupied molecular orbital (HOMO and LUMO) states for the isolated molecules are presented in Figs 1 and 2. These have been obtained with standard density functional theory (DFT) in the local spin-density approximation (LSDA)[11]. Besides their different HOMO–LUMO gaps, which are about 5 eV in octane and about 2.5 eV in tricene, the HOMO and LUMO states possess distinct characteristics. In octane, the charge density of both the HOMO and the LUMO states has a predominant amplitude around the sulphur atoms of the thiol group, with little density on the central carbon backbone. In contrast the HOMO and LUMO states of tricene are delocalized throughout the whole molecule with charge density concentrated both on the end-groups and on the central phenyl groups. We therefore expect octane and tricene to form respectively tunnelling and metallic-like spin-valves.

We model a spin-valve by sandwiching the molecule between two semi-infinite nickel contacts, whose magnetization vectors are either parallel (P) or antiparallel (AP) to each other. The two magnetic contacts are also used as current and voltage probes. Here we consider Ni (001) surfaces terminated with a pyramid of nickel atoms. The molecules are then attached to the hollow site of the nickel surface by the thiolate group. Although a multitude of other anchoring situations may be present in actual samples, this

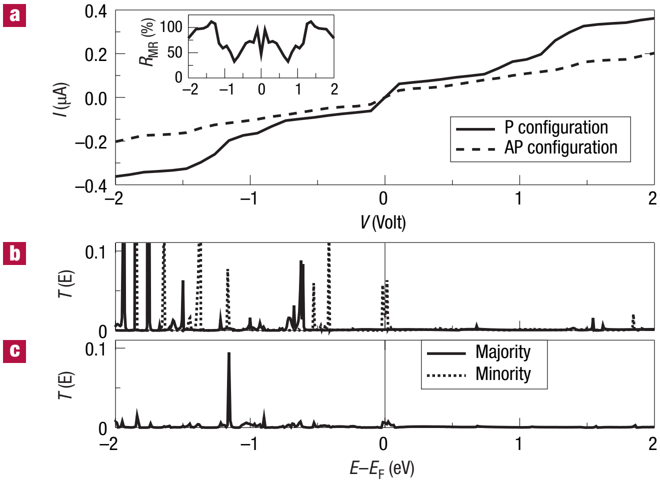

Figure 3 **Magneto-transport properties of a Ni(001)/octane/Ni(001) spin-valve.** **a**, Current–voltage (*I–V*) characteristic, and zero-bias transmission coefficients (*T*(*E*)) for the **b**, parallel and **c**, antiparallel configuration of an octane-based nickel spin-valve. In the antiparallel case the transmission coefficient is identical for both the spin directions. In the inset we show the corresponding magnetoresistance ratio. E_F is the position of the Fermi level of the nickel leads.

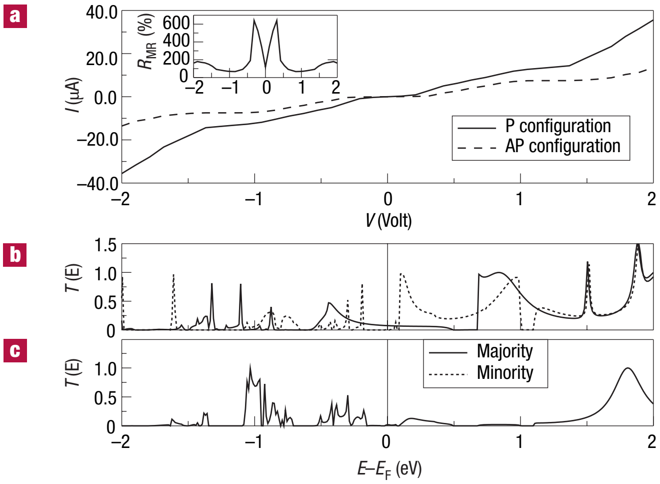

Figure 4 **Magneto-transport properties of a Ni(001)/tricene/Ni(001) spin-valve.** **a**, *I–V* characteristic, and zero-bias transmission coefficients (*T*(*E*)) for the **b**, parallel and **c**, antiparallel configuration of a tricene-based nickel spin-valve. In the antiparallel case the transmission coefficient is identical for both the spin directions. In the inset we show the corresponding magnetoresistance ratio. E_F is the position of the Fermi level of the nickel leads.

seems to be the most stable for the thiolate group on (001) Ni (ref. 12). We always relax the atomic coordinates of the anchor by DFT conjugate gradient molecular dynamics[11] with a tolerance on the forces of 0.01 eV Å^{-1}.

The current–voltage (*I–V*) characteristics of the spin-valves are calculated with a combination of DFT and a non-equilibrium Green's function (NEGF) method[13–15], using a local approximation to the exchange correlation potential (either the LSDA or the generalized gradient approximation GGA). For DFT, we used the pseudopotential localized atomic orbital code SIESTA[11], integrated into our NEGF code[16,17] to yield the versatile *ab initio* transport code SMEAGOL. For details, see Methods; here we just wish to point out that SMEAGOL has been specifically designed for spin-polarized calculations.

In Figs 3 and 4 we present the *I–V* characteristics and the zero-bias transmission coefficients in the parallel and antiparallel configurations, respectively, for the octane and the tricene molecules. In the inset of the *I–V* curves, we show the corresponding bias-dependent magnetoresistance ratio R_{MR} which is defined as $R_{MR} = (I_P - I_{AP})/I_{AP}$, with I_P (I_{AP}) the current in the parallel (antiparallel) state. At zero bias, where all the currents vanish, R_{MR} is calculated using the zero-bias conductances.

From the figures it is clear that both the molecules can form spin-valves with a large magnetoresistance, reaching 600% in the case of tricene. This is a remarkable result in itself, as it demonstrates the viability of the molecular approach to spintronics.

At a more detailed level, it is clear that the two molecules possess rather different characteristics. In the case of octane, the resistance is of the order of 10 MΩ with a current of about 150 nA at 1 V. This is in the same range as in recent experiments on octane-based nickel spin-valves[6], although a direct comparison is difficult because the precise number of molecules bridging the two electrodes is unknown. However, the good agreement in terms of resistance gives us confidence in the ability of our method to describe these devices. The largest contribution to the current comes from a sharp resonance of the transmission coefficient at the Fermi level (see Fig. 3). This is mainly given by minority electrons and it is strongly suppressed in the antiparallel case. Because in the antiparallel configuration the transmission coefficient is essentially zero at any energy around the Fermi energy E_F, we can conclude that the suppression of the aforementioned peak is the main reason for the magnetoresistance.

A closer look at the orbital-resolved density of states of the conduction peak at E_F reveals that this is mainly due to Ni *d* and S *p* orbitals. Furthermore, isosurface plots of the local density of states at the Fermi level show that the charge density is concentrated around the sulphur atoms and little density spreads over the carbon molecular backbone. The plots appear similar to those corresponding to the octane HOMO and LUMO states of Fig. 1, although a precise identification is difficult. This suggests that the transport is tunnelling-like through a Ni *d*–S *p* surface state. To sustain this hypothesis we have calculated the transmission coefficient *T* at zero bias for various *n*-alkane molecules as a function of the number of carbon atoms n ($n = 4, 6, 8$ and 10). This reveals an exponential decay $T \propto \exp(-\beta n)$ with exponent $\beta \approx 0.88$, which clearly demonstrates that we are in a tunnelling regime. It is interesting to note that such an exponent is similar to that found for the same molecules attached to gold (111) surfaces[18]. In addition we observe that the S atoms anchoring the octane molecule possess an induced magnetic moment of $0.07\mu_B$ oriented in the same direction as the nickel magnetization. The presence of charge density at the sulphur atoms is also a feature found for 8-alkane-dithiolate on (111) gold surfaces, and is related to the fact that the Fermi level lies in the molecular HOMO–LUMO gap[18].

The resulting tunnelling magnetoresistance is bias-dependent and varies between 40% and 100%. These values are larger than those found in actual devices[6], where spin-flip and electron–phonon scattering, misalignment of the magnetization of the contacts and current shortcut through highly conductive pinholes can greatly reduce R_{MR}. For this reason our results should be taken as an upper bound for the achievable magnetoresistance in octane-based tunnelling junctions. Finally, some variations in the magnetoresistance ratio are expected when considering different crystalline orientations of the leads, because the bonding properties between the leads and the molecule may change.

The situation for tricene-based spin valves is rather different. In this case the transport is through extended states delocalized over the entire molecule and the typical transmission coefficients approach unity. The resistance of such a device is therefore in the 10-kΩ range. In the parallel case, the zero-bias conductance is dominated at the Fermi level by majority spins, with negligible contribution from the minority electrons. The minority spin conduction starts at about 0.1 eV above E_F and is dominant for energies up to 0.6 eV. At higher energies the transmission coefficient becomes spin-independent because only the unpolarized *s* electrons are available in the leads.

In the antiparallel case there is a general suppression of the transmission coefficient at any energy. For energies close to the Fermi level, this appears as a convolution of the transmission coefficients of the majority and minority spins in the parallel case. The conductance at the Fermi level is therefore small, and the current shows a tiny zero-conductance plateau around zero bias with a consequent very large magnetoresistance ratio, exceeding 600%. We have made additional calculations for various 1,4-*n*-phenyl-dithiolate molecules with different n ($n = 1, 2, 3, 4$). In general the features of the zero-bias transmission coefficients are similar and not strongly dependent on the length of the molecule. There is a reduction of the transmission with length, although the decay is certainly not exponential as in the case of the alkanes, and most importantly the high transmission peaks around the Fermi level remain.

The features of the transmission coefficient can be qualitatively understood in terms of transport through a single molecular state. Let $t^{\uparrow}(E)$ be the majority spin hopping integral from one of the leads to the molecular state, and $t^{\downarrow}(E)$ the same quantity for the minority spins. Then neglecting multiple scattering from the contacts, the total transmission coefficients of the entire spin-valve in the parallel state can be written $T^{\uparrow\uparrow}(E) = (t^{\uparrow})^2$ and $T^{\downarrow\downarrow}(E) = (t^{\downarrow})^2$ respectively for the majority and minority spins. Similarly the transmission in the antiparallel configuration is $T^{\uparrow\downarrow}(E)=T^{\downarrow\uparrow}(E)=t^{\uparrow}t^{\downarrow}$. Thus $T^{\uparrow\downarrow}(E)$ is a convolution of the transmission coefficients for the parallel case $T^{\uparrow\downarrow} \propto (T^{\uparrow\uparrow}T^{\downarrow\downarrow})^{1/2}$.

This qualitative argument gives us a tool for understanding the magnetoresistance and reproduces the main features of the transmission coefficients. For the case in which only one spin couples to the molecular state, the total transmission in the antiparallel case will be identically zero because either $t^{\uparrow}$ or $t^{\downarrow}$ vanishes. This is the most desirable situation in real devices because, in principle, an infinite R_{MR} can be obtained. Furthermore if for a particular energy window the transport is through two distinct molecular states, which are respectively coupled to the majority and minority spin only, then in this window one will find $T^{\uparrow\uparrow}(E) \neq 0$, $T^{\downarrow\downarrow}(E) \neq 0$ but $T^{\uparrow\downarrow}(E) = 0$. This situation is present in tricene for energies between 0.5 eV and 1.0 eV above E_F.

We now discuss the nature of the molecular states involved in the transmission around the Fermi level. In general one expects the conductance to be dominated by resonant transport either through the HOMO or the LUMO state of the molecule[19]. This results in peaks in the zero-bias transmission coefficient as a function of energy, and usually one is able to identify those corresponding to the HOMO and LUMO gap. In the case of 1,4-phenyl-dithiolate with gold electrodes, the HOMO–LUMO peaks are clearly visible and well separated[19]. In contrast, for the 1,4-tricene-dithiolate with nickel studied here the situation seems different. In fact the transmission coefficients for the parallel case show two peaks respectively for majority and minority spins with a separation of only 0.5 eV, not corresponding to the HOMO–LUMO gap.

To identify these states we have followed the evolution of the orbital-resolved density of states (DOS) for a tricene molecule attached to nickel as a function of the Ni–S separation. In particular we have investigated the dependence of the carbon *p* and sulphur *p* DOS, because these are the relevant orbitals for the bonding to the nickel surface. This is presented in Fig. 5. From the figure one notices that the two sulphur *p* HOMO states of the isolated tricene molecule steadily spin-split and broaden as the Ni–S distance is decreased. At the equilibrium position (1.28 Å) the broadening is large, although at the Fermi level one can still identify two sulphur *p* states for the majority spin (–0.5 eV and 0.1 eV from E_F) and one for the minority (0.1 eV from E_F). We can then conclude that the transport is through a very broadened HOMO state. Also, in tricene molecules the sulphur atoms posses a tiny spin-polarization, which is a further indication of strong coupling.

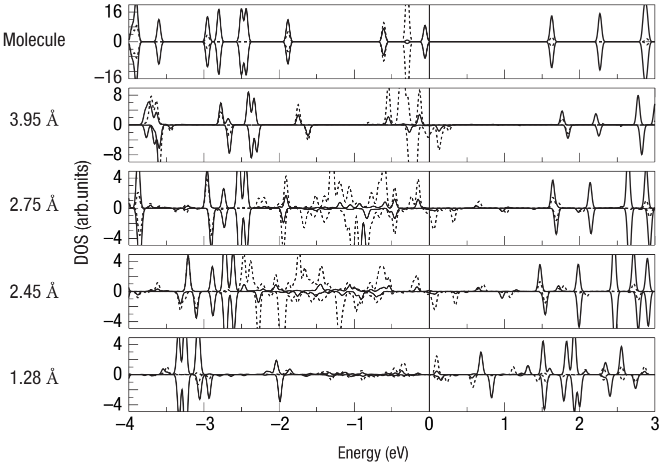

Figure 5 **Orbital-resolved density of states for a tricene molecule attached to nickel electrodes as a function of the distance between the sulphur atom and the nickel hollow site.** The solid and dashed lines are respectively for the carbon *p* and sulphur *p* DOS. The vertical line denotes the position of the Fermi level ($E_F = 0$).

The non-trivial behaviour of the DOS with the Ni–S separation suggests that engineering the end-groups is a crucial factor for tuning the magnetoresistance. We have therefore considered tricene molecules terminated with selenium instead of sulphur. As the atomic radius of the terminating atom T increases the Ni–T distance becomes bigger. This results in a smaller broadening of the transmission peaks with a consequent strong reduction of the zero-bias conductance of the antiparallel case, and a marked increase in the magnetoresistance ratio. In the cases studied the Ni–T separation goes from 1.28 Å to 1.46 Å and the zero-bias magnetoresistance ratio from 600% to 700% when changing from S to Se.

Our two cases, with different specific molecules forming the spin valves, convincingly demonstrate that molecular spin valves can yield large magnetoresistance ratios. For the case of octane molecules the transport is tunnelling-like and magnetoresistances of the order of 100% can be achieved, in good agreement with recent experimental data[6]. In contrast, for the case of transport through molecular states extending throughout the entire molecule (tricene), much larger magnetoresistance ratios can be achieved. This is the result of the strong current suppression in the antiparallel configuration due to the spin-selective coupling of the molecule to the leads. The effect can be tuned by end-group engineering, paving the way to a 'chemical' approach to spintronics.

METHODS

Our main theoretical tool is the code SMEAGOL (spin and molecular electronics in an atomically generated orbital landscape; www.smeagol.tcd.ie), which combines the non-equilibrium Green's function (NEGF) method[13–15] with the DFT code SIESTA[11].

Following Caroli *et al.*[14] we break our two terminal device into three regions, namely two semi-infinite voltage/current leads and an 'extended molecule' region containing the molecule and part of the leads. The number of atomic planes of the contacts to include in the extended molecule depends on the screening length of the metal forming the leads, and the general rule is that the charge density of the most external plane of the extended molecule matches that of the bulk electrodes. The central quantity is then the retarded Green's function for the extended molecule, which reads

$$\mathbf{G} = \lim_{\eta\to 0+}[(\varepsilon + i\eta) - \mathrm{H}_s - \Sigma_L - \Sigma_R{}^{-1}]$$

where ε is the energy, H_s is the hamiltonian matrix of the extended molecule, and Σ_L and Σ_R are the self-energies respectively of the left- and right-hand-side leads. These are energy-dependent matrices that carry all the information about the electronic states of the leads, their occupation and eventually the bias, and allow us to transform an infinite open problem into an energy-dependent finite one. The self-energies are in general non-hermitian quantities, which means that the number of electrons in the extended molecule is not conserved, and therefore charging effects can be efficiently described.

From the Green's function **G** one can extract the density matrix ρ, and hence construct a new DFT hamiltonian matrix[16]. Finite bias can be introduced at any iteration as a rigid shift of the chemical potential of the two leads plus a linear potential ramp in the Hartree potential of the extended molecule. In our present case this is done in *k*-space by using the fast Fourier-transform scheme. This procedure is iterated until it reaches self-consistency when the total transmission coefficient is extracted using a Landauer-like formula[16]. Although the scattering potential is calculated self-consistently, no inelastic effects are included. Therefore the transport is entirely phase-coherent and there is no energy dissipation in the junction. This is a good approximation in the limit of low temperature and small bias, conditions that are usually met in molecular spin-valve experiments[6].

Although the method is similar to other state-of-the-art DFT-based quantum transport algorithms[20,21], to our knowledge SMEAGOL is the only fully spin-polarized code available at present. This goes beyond the use of spin-polarized exchange correlation potentials, including the non-collinear spin option, because magnetic materials carry additional difficulties with respect to non-magnetic systems. In fact the localized *d* electrons co-exist in the valence with the extended *s* electrons, making the hamiltonian matrix rather sparse. In this situation conventional recursive methods[13] have problems in converging the surface Green's functions of the leads, which are essential to construct the self-energies[13–16]. In SMEAGOL, surface Green's functions are calculated using our semi-analytical expression[17], after having regularized the hamiltonian matrix with a combination of generalized single-value decomposition and gaussian elimination schemes.

CALCULATIONS

Going to the details of our calculations, we always construct the unit cell of the extended molecule including four nickel atomic planes on each side, for a total of 40 nickel atoms. We use standard scalar relativistic pseudopotentials with the following reference configurations: H $1s^12p^03d^0$, C $2s^22p^23d^0$, S $2s^22p^43d^0$ and Ni $4s^14p^03d^9$. Furthermore, for good convergence we need to consider a rather rich basis set. For both the molecules we have used a single zeta basis for H, C and S *s* orbitals, double zeta for Ni *s*, *p* and *d*, and double zeta polarized for C and S *p* orbitals[11]. This basis gives us a hamiltonian with over a thousand degrees of freedom. Finally the charge density is obtained by integrating the Green's function over 50 imaginary and 600 real energy points according to the scheme described in ref. 16.

Received 18 August 2004; accepted 19 January 2005; published 6 March 2005.

References

1. Wolf, S. A. *et al.* Spintronics: a spin-based electronics vision for the future. *Science* **294**, 1488–1495 (2001).
2. Tsukagoshi, K., Alphenaar, B. W. & Ago, H. Coherent transport of electron spin in a ferromagnetically contacted carbon nanotube. *Nature* **401**, 572–574 (1999).
3. Ouyang, M. & Awschalom, D. D. Coherent spin transfer between molecularly bridged quantum dots. *Science* **301**, 1074–1078 (2003).
4. Xiong, Z. H., Wu, D., Valy Vardeny, Z. & Shi, J. Giant magnetoresistance in organic spin-valves. *Nature* **427**, 821–824 (2004).
5. Dediu, V., Murgia, M., Matacotta, F. C., Taliani, C. & Barbanera, S. Room temperature spin polarized injection in organic semiconductor. *Solid State Commun.* **122**, 181–184 (2002).
6. Petta, J. R., Slater, S. K. & Ralph, D. C. Spin-dependent transport in molecular tunnel junctions. *Phys. Rev. Lett.* **93**, 136601 (2004).
7. Pati, R., Sanapati, L., Ajayan, P. M. & Nayak, K. First-principles calculations of spin-polarized electron transport in a molecular wire: molecular spin valve. *Phys. Rev. B* **68**, 100407(R) (2003).
8. Emberly, E. G. & Kirczenow, G. Molecular spintronics: spin-dependent electron transport in molecular wires. *Chem. Phys.* **281**, 311–324 (2002).
9. Kim, G.-H. & Kim, T.-S., Electronic transport in single-molecule magnets on metallic surfaces. *Phys. Rev. Lett.* **92**, 137203 (2004).
10. De Teresa, J. M. *et al.* Inverse tunnel magnetoresistance in Co/$\mathrm{SrTiO_3/La_{0.7}Sr_{0.3}MnO_3}$: new ideas on spin-polarized tunnelling. *Phys. Rev. Lett.* **82**, 4288–4291 (1999).
11. Soler, J. M. *et al.* The SIESTA method for *ab initio* order-*N* materials simulation. *J. Phys. Condens. Matter* **14**, 2745–2779 (2002).
12. Mullins, D. R. *et al.* The adsorption site and orientation of $\mathrm{CH_3S}$ and sulfur on Ni(001) using angle-resolved X-ray photoelectron spectroscopy. *Surf. Sci.* **372**, 193–201 (1997).
13. Datta, S. *Electronic Transport in Mesoscopic Systems* (Cambridge Univ. Press, Cambridge, 1995).
14. Caroli, C., Combescot, R., Nozieres, P. & Saint-Janes, D. A direct calculation of the tunneling current: IV. Electron–phonon interaction effects. *J. Phys. C* **5**, 21–42 (1972).
15. Ferrer, J., Martín-Rodero, A. & Flores, F. Contact resistance in the scanning tunneling microscope at very small distances. *Phys. Rev. B* **38**, 10113–10115 (1988).
16. Reily Rocha, A. & Sanvito, S. Asymmetric *I–V* characteristics and magnetoresistance in magnetic point contacts. *Phys. Rev. B* **70**, 094406 (2004).
17. Sanvito, S., Lambert, C. J., Jefferson, J. H. & Bratkovsky, A. M. General Green's-function formalism for transport calculations with *spd* Hamiltonians and giant magnetoresistance in Co- and Ni-based magnetic multilayers. *Phys. Rev. B* **59**, 11936–11948 (1999).
18. Tomfohr, J. K. & Sankey, O. F. Complex band structure, decay lengths, and Fermi level alignment in simple molecular electronic systems. *Phys. Rev. B* **65**, 245105 (2002).
19. Di Ventra, M., Pantelides, S. T. & Lang, N. D. First-principles calculation of transport properties of a molecular device. *Phys. Rev. Lett.* **84**, 979–982 (2000).
20. Brandbyge, M., Mozos, J.-L., Ordejón, P., Taylor, J. & Stokbro, K. Density-functional method for non-equilibrium electron transport. *Phys. Rev. B* **65**, 165401 (2002).
21. Taylor, J., Guo, H. & Wang, J. *Ab initio* modeling of quantum transport properties of molecular electronic devices. *Phys. Rev. B* **63**, 245407 (2001).

Acknowledgements

This work is sponsored by the Science Foundation of Ireland under the grant SFI02/IN1/I175, the UK EPSRC and the EU network MRTN-CT-2003-504574 RTNNANO. J.F. and V.M.G.S. thank the Spanish Ministerio de Educacíon y Ciencia for financial support (grants BFM2003-03156 and AP2000-4454). A.R.R. thanks Enterprise Ireland (grant EI-SC/2002/10) for financial support. Travel has been sponsored by the Royal Irish Academy under the International Exchanges Grant scheme. We thank J. H. Jefferson for discussions.
Correspondence and requests for materials should be addressed to S.S.

Competing financial interests

The authors declare that they have no competing financial interests.